Attenuated Total Reflection of the Rubidium D₂ Line in Optically Dense Vapor

Satoshi Tojo, Yuuki Murakami, Masahiro Hasuo and Takashi Fujimoto

Department of Engineering Physics and Mechanics, Graduate School of Engineering, Kyoto University, Kyoto 606-8501

Absorption spectrum of the evanescent light at a glass/Rb vapor interface has been observed with atom density from 9×10^{19} m^{-3} to 5×10^{20} m^{-3}. Absorption is as high as 60% at the peak of a hyperfine structure split line. The absorption spectrum of the experiment is compared with that of the calculation based on Fresnel's relation on the assumption of a homogeneous electric susceptibility of the vapor. Near the critical angle the calculation which incorporates the Lorentz–Lorenz local-field correction reproduces the experimental red shift only partly.

1. Introduction

Reflection spectroscopy at a dielectric/vapor interface is sensitive to a thin vapor layer near the dielectric surface within a thickness of the order of the light wavelength. For the case of the normal incidence of the light to the interface which is called the selective reflection a sub-Doppler structure has been observed, which is due to the transient behavior of atoms leaving the surface after a collision on the surface.[1,2] From the observation of the line profile of this sub-Doppler structure, the van der Waals interaction between an atom and a surface has been investigated.[3,4] Another reflection spectroscopy is based on attenuated total reflection (ATR) in which the evanescent light gives rise to absorption.[5] In this method the thickness of the vapor layer for absorption is determined by the angle of incidence of the light to the dielectric surface. Collision dynamics of atoms in the vicinity of a surface has been investigated by this method.[6]

One of the advantages of the reflection spectroscopy is that it can offer information about an optically dense vapor, to which conventional transmission spectroscopy is not applicable. The broadening and the shift of the selective reflection spectra were observed on a dense rubidium vapor and the atom–atom interaction was investigated.[4] The atom number density of a rubidium vapor near a surface was evaluated from the ATR spectrum.[7] However, for an optically very dense vapor, a conventional scheme of the light reflection at the dielectric/vapor interface may become inadequate. In the selective reflection, the interaction between atoms and the light field in the optically dense vapor results in a non-exponential decay of the intensity of light.[8] Thus, the selective reflection spectra are modified, and the shift of the absorption line is observed. Such an effect on ATR, however, has not been observed experimentally or discussed theoretically so far.

In this report, we present our measurement of the ATR spectra with an optically dense rubidium vapor, in which the light frequency dependence of the refractive index and the propagation of the evanescent light in the vapor becomes substantial near the critical angle.[7,9]

2. Experiment

Figure 1 shows the schematic diagram of our experimental setup. The light source is an external-cavity
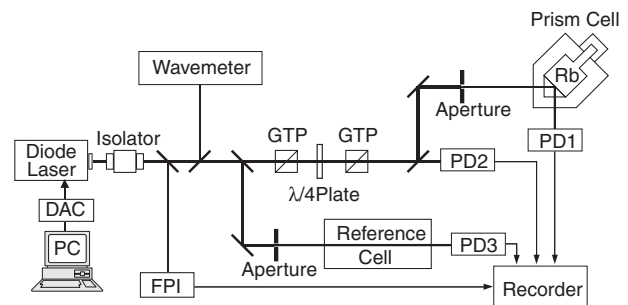

Fig. 1. The experimental setup. FPI: Fabry–Pérot interferometer as a frequency marker, GTP: Glan–Thompson prism, PD: photo detector, DAC: digital-to-analog converter.

controlled diode laser (EOSI 2010), which has the output power up to 18 mW and the spectral line width of 100 kHz at the wavelength of 780 nm. We scan the laser light frequency over the rubidium D₂ line by sweeping the voltage applied to the piezoelectric element which controls the external cavity. After passing through an optical isolator a part of the light beam is incident on a Fabry–Pérot frequency marker with the free spectral range of 1.870 ± 0.004 GHz; we have calibrated this value against the separation (1.124 GHz) between the ^{85}Rb$(F = 3 \rightarrow F' = 4)$ peak and the ^{87}Rb$(F = 2 \rightarrow F' = 3)$ peak in the saturated absorption spectrum using a 5 cm long reference rubidium cell at the room temperature. Another portion of the laser light is led to a wavemeter (Burleigh Instrument, WA4500D). The main part of the laser beam goes through a Glan–Thompson prism and a quarter wave plate. The light is thus circularly polarized. By another Glan–Thompson prism, the laser light is polarized horizontally (p-polarization) or vertically (s-polarization) with almost equal intensity. It goes through an aperture (1 mm in diameter) and is incident on the prism of Pyrex glass whose refractive index is 1.472 at 780 nm, giving the critical angle of 42.79°. This prism serves as one side of the cell, which contains a rubidium vapor. This cell, which is called the prism cell hereafter, is enclosed by a cover cell whose entrance and exit windows are wedged to eliminate the interference between the reflected light by the outer and inner surfaces. The main body of the prism cell and the leg (20 mm long) on the opposite side to the prism are heated independently, so that the temperature of the main

body is uniform and the leg served as the coldest point which determines the vapor pressure of rubidium. The heater wire are wound in such a way that the induced magnetic fields almost cancel in the cell. The intensity of the laser light beam incident on the prism is $16\,\mu W/mm^2$. The incident angles to the prism are $43.5 \pm 0.05°$ and $50 \pm 0.06°$. The incident angles are determined with respect to the back-reflection of the normal incident light on the outer surface of the $45°$ prism. Another method is to use the relative angles with respect to the critical angle; the critical angle is determined from the change of reflection spectra from the partial reflection spectrum to the total reflection one. The totally reflected light is detected by a photodiode (Hamamatsu, S1336-5KB) (PD1). In order to normalize the reflected light intensity, a part of the laser light is detected by a photodiode (PD2). Another part of the laser light goes through the reference cell at the room temperature and is detected by a photodiode (PD3). Outputs of the photodiodes are registered by a digital recorder.

Figure 2 shows an example of raw date of the outputs of the photodiodes and the frequency marker. The incident angle is $50°$. The temperatures of the main body and the coldest point of the prism cell are $493\,K$ and $463\,K$, respectively. Figure 3 shows the energy level diagram of the rubidium D_2 line with the hyperfine splitting. The isotope of ^{85}Rb having nuclear spin of $5/2$ occupies 72.2% of natural rubidium, and 27.8% is ^{87}Rb with nuclear spin $3/2$. The four absorption peaks in Fig. 2 correspond to the

hyperfine structure splitting of the ground state $5^2S_{1/2}$. The splittings of the upper levels are too small to be separated in the present experiment; the Doppler width is $511\,MHz$ for $300\,K$.

When we changed the intensity of the incident laser light from $2\,\mu W/mm^2$ to $32\,\mu W/mm^2$, no appreciable difference was observed in the spectra in any respects except for the statistical fluctuations. Thus, our experiment was free from any saturation effect. We also made a measurement with the heater current cut off just before the measurement. No appreciable change was detected. Thus, we eliminated possible effects by the magnetic field induced by the heater current. The scan of the laser frequency was found to be non-uniform, so that a polynomial function was fitted to the position of the marker. By combining the free spectral range of the marker and the fitted polynomial, we plotted our spectrum on the frequency scale.

3. Results and Discussion

The thick solid curves in Fig. 4 show the measured ATR spectra at the incident angle $50°$ for the p-polarization (a) and the s-polarization (b). The temperatures of the coldest point are set at 423, 443 and 463 K with the accuracy of 5 K. Throughout the measurement, the main body of the prism cell is kept at $493\,K$. The ratio between the absorption intensity for the p-polarization and that for the s-polarization is almost $2:1$, which is consistent with the result of the similar measurement at 390 K by Kiersnowski *et al.*[10] The broader line profile of the ATR spectra than that of the transmission spectrum of the reference cell is seen; this originates mainly from the broader Doppler width owing to the higher temperature of the prism cell. It is also well-known that the pseudo-momentum of the evanescent light
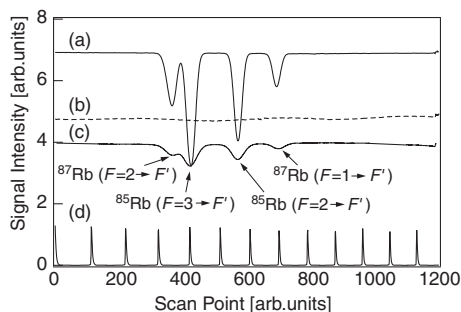

Fig. 2. An example of raw data. (a) the laser light intensity transmitted through the reference cell at 300 K, (b) the laser light intensity measured by PD2, (c) the laser light intensity reflected by the prism cell, (d) the output of the frequency marker. The incident angle of the laser beam is $50°$. The temperatures of the main body and the coldest point of the prism cell are 493 K and 463 K, respectively.
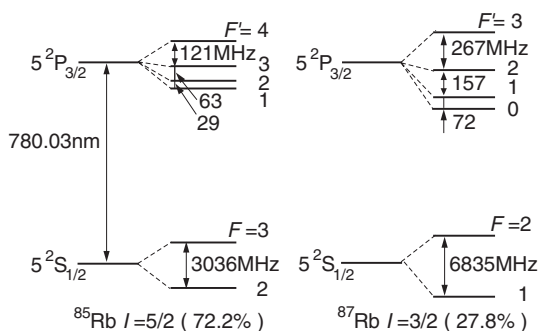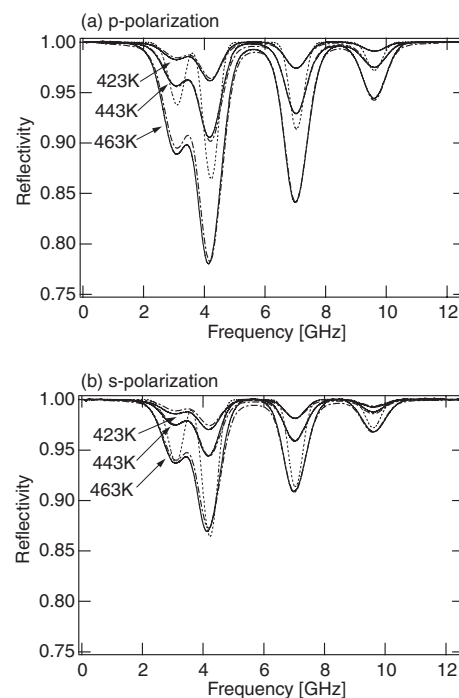

Fig. 3. Energy level diagram with the hyperfine splitting of the Rb D_2 line.

Fig. 4. The ATR spectra at the incident angle of $50°$ for (a) the p-polarization and (b) the s-polarization. The dash–dot curves are the calculated spectra. The dotted curve is the measured transmission spectrum of the reference cell.

field and the transit time broadening due to its short penetration depth contribute to the broadening.[9,11)] We calculate the reflection spectra by using the model based on Fresnel's relation of reflection assuming a homogeneous electric susceptibility of the vapor.[7,9)] The reflectivity R is defined as $R = |r|^2$ with the amplitude reflection coefficients r. Coefficients r_p for the p-polarization and r_s for the s-polarization are expressed by Fresnel's law,

$$r_p = \frac{n_1 \cos\theta_i - (n_1/n_2)^2 \sqrt{n_2^2 - n_1^2 \sin^2\theta_i}}{n_1 \cos\theta_i + (n_1/n_2)^2 \sqrt{n_2^2 - n_1^2 \sin^2\theta_i}}, \qquad (1)$$

$$r_s = \frac{n_1 \cos\theta_i - \sqrt{n_2^2 - n_1^2 \sin^2\theta_i}}{n_1 \cos\theta_i + \sqrt{n_2^2 - n_1^2 \sin^2\theta_i}}, \qquad (2)$$

where θ_i is the incident angle of the light and n_1 and n_2 are the refractive index of the glass and that of the vapor, respectively. The latter is related to the electric susceptibility $\chi(\omega)$[9)]

$$n_2(\omega) = \sqrt{1 + \chi(\omega)}$$
$$= \left(1 + \frac{N f_n e^2}{\epsilon_0 m} \frac{1}{2\omega} \int_{-\infty}^{\infty} dv_x \int_0^{\infty} dv_z \frac{W(v_x, v_z)}{\Delta(\omega) - \alpha k_0 v_x - i(\gamma + \eta k_0 v_z)}\right)^{1/2}, \qquad (3)$$

with

$$\eta = i\sqrt{1 - n_1^2 \sin^2\theta_i}, \quad \alpha = n_1 \sin\theta_i, \qquad (4)$$

where η and α are coefficients which express the transit-time-broadening and the pseudo-momentum, respectively, W is the normalized Maxwell distribution function, $\Delta(\omega)$ is the detuning frequency of the light ω from the resonance, γ is the natural width, k_0 is the wave vector in vacuum, N is the density of the vapor, f_n is the oscillator strength, v_x and v_z are components of atom velocity parallel and perpendicular to the surface, respectively, ϵ_0 is the dielectric constant of vacuum, e is the elementary electric charge and m is the electron mass. In the calculation, we include the effects of the pseudo momentum, the transit time broadening and the short penetration depth of the evanescent light, which are substantial at large incident angles. We also include the Lorentz–Lorenz local-field correction,[5,8)] which may not be negligible in an optically dense medium. The only adjustable parameter is the atom density. The agreement between the calculated absorption spectra and the experiment is satisfactory. We obtain atom densities 8.68×10^{19}, 1.95×10^{20} and 4.73×10^{20} m^{-3} at 423, 443 and 463 K, respectively. These densities are lower by about 30% than those given from Killian's empirical formula,[12)] and are consisted with Zhao *et al.*[7)]

From the comparison between the transmission spectrum of the reference cell and the ATR spectra, we recognize the red shift of the absorption lines, especially those of ^{85}Rb, in the ATR spectra for both the s- and p-polarizations. The magnitude of the shift is almost the same for the s- and p-polarizations at the same temperature. The shifts are reproduced partly in the calculation. Since the shift is due to the frequency dependent refractive index of the vapor, the effect should be larger near the critical angle.[7,9)] Figure 5 shows the ATR spectra at the incident angle of 43.5°. The red shift is even more salient. The shift increases with the increase not only in the atom density but also in the absorption intensity; in the ^{85}Rb($F = 3 \to F'$) transition the ratio of shift (394 MHz) at 463 K to that (151 MHz) at 423 K is 2.6 for the p-polarization at 43.5°, while that is 1.7 (89 MHz/52 MHz) at 50°. Uncertainties of the experimental shifts are ~1 MHz derived from both the transmission

spectra and the reflection spectra fitted to Voigt functions.

We see a discrepancy in the absorption intensity between the experiment and the calculation in Fig. 5(a). The discrepancy may be due to a small error in the incident angle because the magnitude of the absorption intensity depends strongly on the incident angle near the critical angle. If the angle were larger by 0.2°, the difference would be explained for p-polarization. However, there would be still inconsistency since the adjustment causes a discrepancy for s-polarization.

We consider the red shift of 394 MHz at 463 K for p-polarization at 43.5° in the ^{85}Rb($F = 3 \to F'$) transition. The shift may be explained as due to the frequency
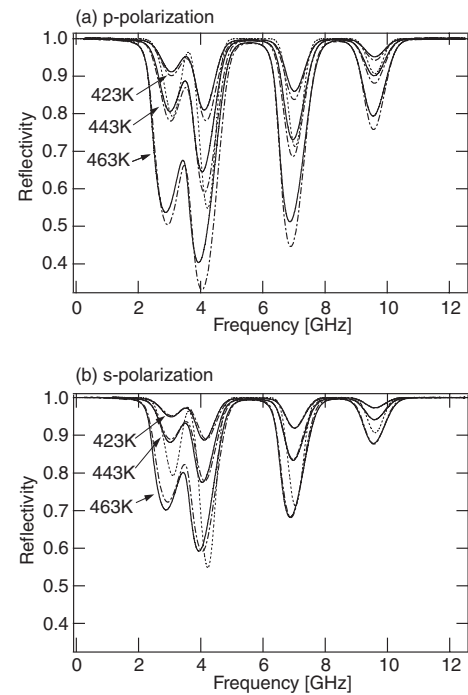
Fig. 5. The ATR spectra at the incident angle of 43.5° for (a) the p-polarization and (b) the s-polarization. The dash–dot curves are the calculated spectra. The dotted curve is the measured transmission spectrum of the reference cell.

dependence of the refractive index of the vapor. In our calculation based on Fresnel's relation contains the complex refractive index of the vapor.[5] In a dilute vapor the peak of absorption is not shifted since absorption is approximately proportional to $Im[\chi(\omega)]$ in the conventional scheme. In a dense vapor absorption is proportional to $Re[\sqrt{1 + \chi(\omega)} - n_1^2 \sin^2\theta]$.[5] The red shift calculated from this assumption 176 MHz. We estimate the red shift due to the Lorentz–Lorenz local-field correction.[8] Absorption is then proportional to $Re[\sqrt{1 + 3\chi(\omega)/(3 - \chi(\omega))} - n_1^2 \sin^2\theta]$ in the case. The additional shift is about 8 MHz; this is almost independent of the incident angle. Thus, our calculation cannot fully account for the shift. The residual shift is 210 MHz. In the case of the $^{85}Rb(F = 2 \rightarrow F')$ transition the residual shift is 119 MHz; in the $^{87}Rb(F = 1 \rightarrow F')$ transition the shift is 60 MHz. At present we do not have any clear explanation about the discrepancy. Below we discuss possible origins.

Figure 6 shows the components of the wave vector of the light in the rubidium vapor at 463 K obtained from Snell's law. The incident angle is 43.5° (solid lines) and 50° (dotted lines). Here, we define the x-axis along the direction parallel to the surface in the plane of incidence and z-axis along the direction normal to the surface. We use the complex refractive index of the vapor. The absorption in the ATR spectra originates from the real part of k_z, where k_z is the z-component of the wave vector; the absorbed light is the strongly damped propagating light into the vapor. The penetration depth defined as $2\pi/Im(k_z)$ also depends strongly on the incident angle. In the case of the incident angle of 50° $Re[k_z]$ in the $^{85}Rb(F = 2 \rightarrow F')$ and $^{87}Rb(F = 3 \rightarrow F')$ transitions is small by a factor of 30 in comparison with k_x. The real part of wave vector $(k_x, 0, Re[k_z])$ is approximately parallel to x-axis. The conventional Fresnel's calculation reproduce approximately the shift in the experiments as seen in Fig. 4. In the case of 43.5° in dense vapor $Re[k_z]$ is substantial in comparison with k_x. In this case velocity distribution of v_z in eq. (3) is spatially asymmetric about the wave vector while it is symmetric in the case of dilute vapor. Therefore, a conventional scheme of the absorption of the evanescent light by atoms may break down and the contributions from atoms with $v_z > 0$ and $v_z < 0$ may be different.[9]

In the theory of the selective reflection, a low-density limit is defined which is below $Nk^{-3} = 1$ for strongly allowed transitions in alkali metal atoms. Here N is the atom density in the vapor, $k = 2\pi/\lambda$ is the light wave number with the light wavelength λ.[8] If the density is higher than this boundary, the assumption that the light field in the atomic vapor is plane wave of exponentially attenuating amplitude becomes in adequate for the reflected light. The non-exponential decay of the transmitted light results in deformation of the selective reflection spectra.[8] In our case at 463 K, $Nk^{-3} = 0.9$, which is close to this limit. The above calculation based on the Fresnel's relation assuming a homogeneous electric susceptibility may not be justified. Further theoretical investigation is needed.
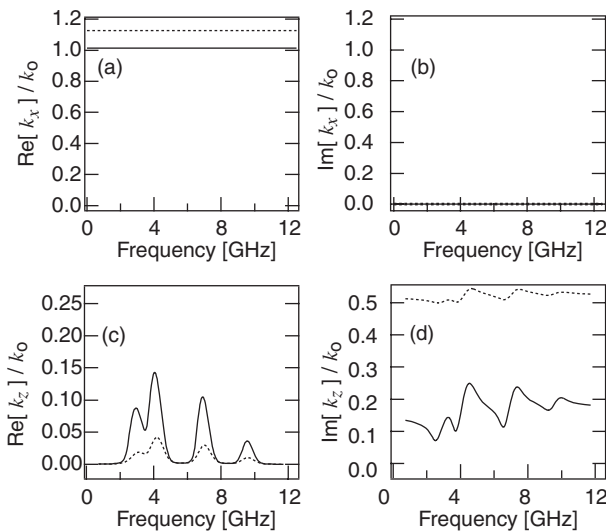
Fig. 6. Wave vector components of the light in the rubidium vapor at the incident angle of 43.5° (solid lines) and 50° (dotted lines) at 463 K calculated from the Snell's law extended to a complex refractive index of the vapor. (a) the real part of k_x, (b) the imaginary part of k_x, (c) the real part of k_z, (d) the imaginary part of k_z.

1) J. L. Cojan: Ann. Phys. (Paris) **9** (1954) 385.
2) M. F. H. Schuurmans: J. Phys. (Paris) **37** (1976) 469.
3) H. Failache, S. Saltiel, M. Fichet, D. Bloch and M. Ducloy: Phys. Rev. Lett. **83** (1999) 5467.
4) M. Gorris-Neveux, P. Monnot, M. Fichet, M. Ducloy, R. Barbé and J. C. Keller: Opt. Commun. **134** (1997) 85.
5) P. Boissel and F. Kerherve: Opt. Commun. **37** (1981) 397.
6) V. G. Bordo, J. Loerke and H.-G. Rubahn: Phys. Rev. Lett. **86** (2001) 1490.
7) K. Zhao, Z. Wu and H. M. Lai: J. Opt. Soc. Am. B **18** (2001) 1904.
8) J. Guo, J. Cooper and A. Gallagher: Phys. Rev. A **53** (1996) 1130.
9) G. Nienhuis, F. Schuller and M. Ducloy: Phys. Rev. A **38** (1988) 5197.
10) K. Kiersnowski, L. Jorefowski and T. Dohnalik: Phys. Rev. A **57** (1998) R4079.
11) T. Matsudo, H. Hori, T. Inoue, H. Iwata, Y. Inoue and T. Sakurai: Phys. Rev. A **55** (1997) 2406.
12) Reference 7, Eq. (29); $N = 2.570 \times 10^{26} \exp(-9514/T)T$, where T is temperature.